

INTERNATIONAL SOCIETY FOR SOIL MECHANICS AND GEOTECHNICAL ENGINEERING



This paper was downloaded from the Online Library of the International Society for Soil Mechanics and Geotechnical Engineering (ISSMGE). The library is available here:

<https://www.issmge.org/publications/online-library>

This is an open-access database that archives thousands of papers published under the Auspices of the ISSMGE and maintained by the Innovation and Development Committee of ISSMGE.

The paper was published in the proceedings of the 10th International Conference on Scour and Erosion and was edited by John Rice, Xiaofeng Liu, Inthuorn Sasanakul, Martin McIlroy and Ming Xiao. The conference was originally scheduled to be held in Arlington, Virginia, USA, in November 2020, but due to the COVID-19 pandemic, it was held online from October 18th to October 21st 2021.

Pipe Erosion In Laminar Flow

Gijs Hoffmans

Hoffmans Advice, The Hague, The Netherlands; e-mail: hoffmans.advice@outlook.com

ABSTRACT

Particle transport occurs when there is no balance between the wall shear stress of the water in the pipe and the critical shear stress of the material. When the shear stress is less than some critical value, particles remain motionless and can be considered as fully stable. But when it exceeds its critical value, particle motion begins. The incipient motion is difficult to define because of the phenomena that are random in time and space. Here, the incipient motion of particles or pipe erosion is described with the extended Shields diagram for laminar flow and the shear-stress theory as proposed by Grass. Different parameters which describe the erodibility of the sediment are discussed for both fines and coarse sand. To understand pipe erosion beneath clayey river dikes and/or impermeable dams the piping process is briefly explained with hydraulic gradients.

INTRODUCTION

Internal erosion is a dangerous phenomenon as it is one of the most common cause of failure in dikes and one of the leading causes of failures in earth dams. Internal erosion occurs when the hydraulic forces exerted by water are sufficient to detach and move particles through a porous media (cracks and/or pipes). A dike/dam may breach within a few hours after evidence of internal erosion becomes obvious. Internal erosion includes many different processes such as piping, soil contact erosion, or suffusion.

Piping is defined as the development of pipes owing to erosion of particles from downstream and along the upstream line towards the river/reservoir until a continuous pipe is formed. Usually a sand boil can be found at the flood plain or downstream of the dam, but the boil might be hidden under water. In such cases the risk of failure increases since erosion is often not detected until it has advanced to a greater extent.

The outline of this paper is as follows. Piping is discussed with a resistance equation that describes both the critical hydraulic dike gradient or the allowable hydraulic gradient and the critical pipe gradient. Next, the incipient motion of particles is modelled with the extended Shields (1936) diagram for laminar flow and the probabilistic shear stress theory of Grass (1970). When pipe erosion occurs the pipe dimensions and the wall shear stress reach their critical values and thus also the mean pipe velocity, the pipe discharge and the hydraulic pipe gradient. Here these critical parameters are deduced and discussed for both fines and coarse sand.

RESISTANCE MODELLING

In the sand layer, two hypothetical zones (Figure 1) are defined: one close to the pipes (Zone A where there is a dip in the hydraulic gradient) and one far away from the pipes (Zone B where the hydraulic head profile is unaltered). Therefore, in Zone B, the streamlines are assumed to be horizontal, while in Zone A, they are curved, which generates both a horizontal and vertical gradient and hence a flow from deeper layers, until equilibrium is reached.

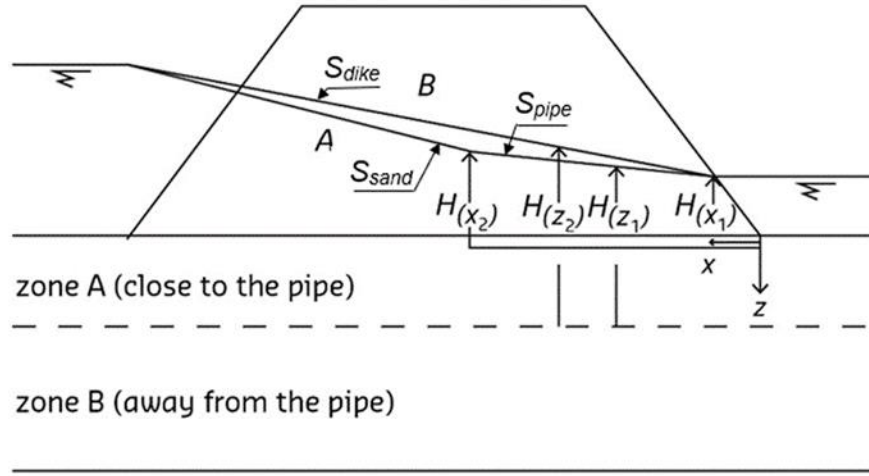


Figure 1. Schematization of sand layer

Computational results of piping at a small scale (e.g., Van Beek, 2015) show that the local gradient is curved both on the entry and on the exit points of the horizontal pipes. Here, these curvatures are linearised, which for field conditions is a reasonable assumption because the length scale of these influence areas is small compared to the long seepage length where the hydraulic pipe gradient is constant. Hence, particularly for prototype situations, the hydraulic dike gradient (S_{dike}) can be divided into two straight curves: the mean hydraulic gradient in the pipes, or the hydraulic pipe gradient (S_{pipe}), and the mean hydraulic gradient upstream of the pipes, or the hydraulic sand gradient (S_{sand}). The gradient S_{dike} is given with ℓ as the pipe length and L as the seepage length:

$$S_{dike} = S_{pipe} + \left(1 - \frac{\ell}{L}\right) (S_{sand} - S_{pipe}).$$

This model implies that the flow in Zone B does not influence the piping mechanism at all. The groundwater flow upstream of the pipes is assumed to be horizontal, and therefore, the hydraulic sand gradient is constant. In the influence zone of the pipe (Zone A, below the pipe), we calculate the groundwater flow towards the pipe, assuming a linear head drop in the pipe and implying that no groundwater flows out. The gradient S_{dike} can also be represented by the following, with $q_{p,m}$ as the pipe discharge per unit width (Hoffmans and Van Rijn 2018):

$$S_{dike} = S_{pipe} + \left(1 - \frac{\ell}{L}\right) \frac{q_{p,m}}{DK}$$

For field conditions, the transmissivity in the sand layer, expressed by DK , is significant larger than the pipe discharge $q_{p,m}$ due to the thickness of the sand layer. Therefore, for dikes and dams the hydraulic dike gradient equals approximately the hydraulic pipe gradient and thus, see also Hoffmans and Van Rijn (2018)

$$S_{dike} \approx S_{pipe}$$

INCIPIENT MOTION OF PARTICLES

The concept of an entrainment threshold is the main issue of sediment transport in theory and practice. The Shields (1936) diagram has been extensively used for determination of incipient conditions for sediment movement problems. The threshold of particle motion is governed by balancing the driving force and the resistance force. The critical mean wall (or bed) shear stress (τ_c) reads, e.g. Van Rijn (2014)

$$\tau_c = \Psi_c (\rho_s - \rho) g d_{50}$$

where d_{50} is the mean particle diameter, g is the acceleration of gravity, ρ is the density of the water, ρ_s is the density of the sediment and Ψ_c is the critical Shields parameter.

The initiation of motion is also influenced by the shape of the particle, for example, whether angular or rounded. However, these effects are not accounted for in the Shields diagram. For fines, say $d_{50} = 0.1$ mm, Shields (1936) found $\Psi_{tur,c} \approx 0.07$ for turbulent flow. Because of pressure fluctuations along the wall, particles in the pipe move more easily in turbulent flow than in laminar flow. Since these turbulence effects are not directly included in the Shields diagram, Ψ_c for the incipient motion of particles under laminar flow conditions is larger than is required under turbulent flow conditions. For laminar flow Mantz (1977) found

$$\Psi_{lam,c} = 0.1 (\text{Re}_{*,c})^{-0.3} \quad \text{for } 0.03 \leq \text{Re}_{*,c} \leq 0.1$$

where $\text{Re}_{*,c} (= k_s u_{*,c} / \nu)$ is the critical shear Reynolds number, k_s is the effective roughness related to the particle diameter or the Nikuradse roughness height ($k_s = 1$ to 5 times d_{50} , d_{84} , or d_{90} according to the literature), $u_{*,c}$ is the critical wall shear velocity and ν is the kinematic viscosity.

An extended Shields diagram was developed by Mantz (1977). Many researchers (e.g. Van Rijn 2014) showed that the critical Shields parameter decreases with an increasing grain size. Figure 2 shows a selection of some tests where the initiation of motion was determined in water. Based on laminar flow tests a relation for $\Psi_{lam,c}$ is proposed ($0.1 \text{ mm} < d_{50} < 0.5 \text{ mm}$) representing general movement of particles (Hoffmans 2020)

$$\Psi_c = \Psi_{lam,c} = 0.2 (D_*)^{-\frac{1}{3}} \quad \text{for } 2 \leq D_* \leq 15 \quad \text{with } D_* = d_{50} \left(\frac{(\frac{\rho_s}{\rho} - 1)g}{\nu^2} \right)^{\frac{1}{3}}$$

where D_* is a dimensionless particle diameter, see also Figure 2, where the computational results and several experiments are plotted.

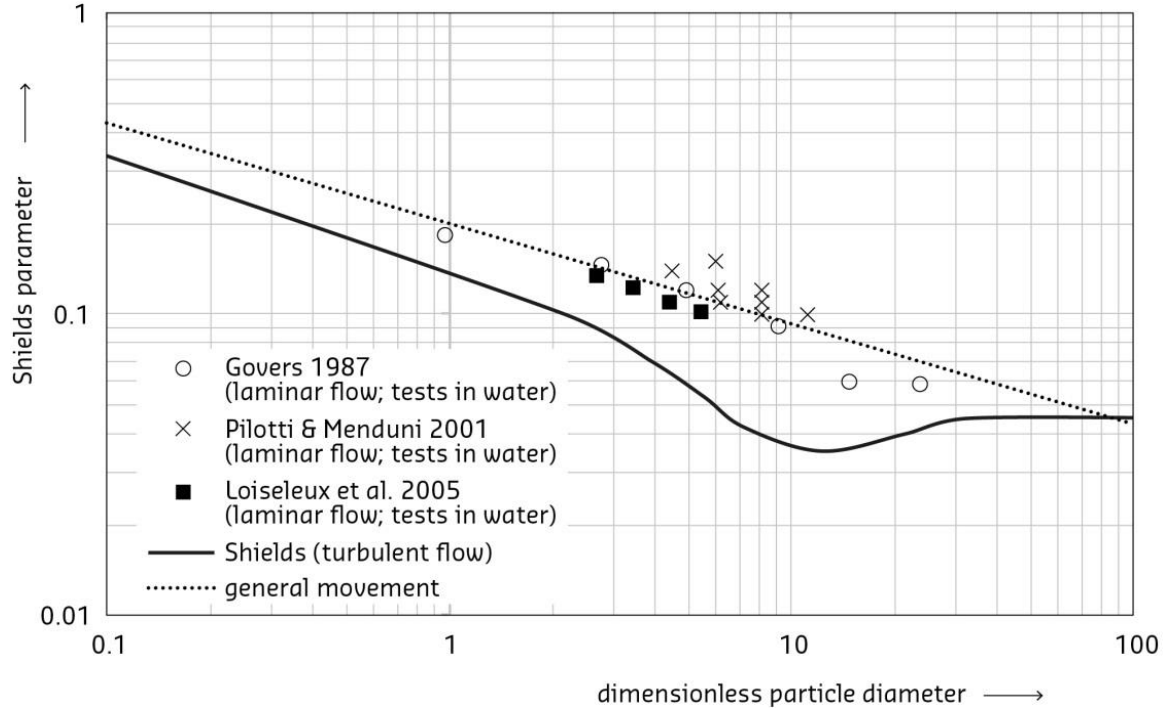


Figure 2. Extended Shields diagram; Ψ versus D^* (Hoffmans 2020)

Particles in the pipes are transported if the mean wall shear stress exceeds a critical value. Here, the erosion resistance is expressed by a critical characteristic wall shear stress (thus pipe erosion starts if $\tau_0 \geq \tau_{c,k}$). For uniform flow and for nearly uniform sediments, the initiation of sediment motion in a pipe is modelled with R as the hydraulic radius and S_{pipe} as the hydraulic pipe gradient (c denotes for critical) as

$$\tau_0 = \rho g R S_{pipe} \geq \tau_{c,k} = \rho g R_c S_{pipe,c}$$

NON-UNIFORMITY OF SAND LAYER

When dealing with particle stability in granular filters, the exact shape of both the shear stress distribution and the critical shear stress distribution is irrelevant. A characteristic value is a value that is higher or lower than the mean value. Usually characteristic values are expressed as a mean value and a fraction of the standard deviation. Hence, the problem of particle stability could be transferred to the magnitude of this fluctuation (e.g. Hoffmans 2012).

As the pipe flow is here assumed to be laminar the influence of wall turbulence is neglected. To include the effects of non-uniform sediments a critical characteristic wall shear stress ($\tau_{c,k}$) is used (see also Grass 1970).

$$\tau_{c,k} = \tau_c - \tau_{RMS,c} \quad \text{with} \quad c_{v,d} = \frac{\tau_{RMS,c}}{\tau_c} \approx 1 - \frac{d_{15}}{d_{50}}$$

Consequently,

$$\tau_{c,k} = \Psi_{\ell am,c}(\rho_s - \rho)gd_{15}$$

where $c_{v,d}$ is the variation ratio representing the effects of the heterogeneity, d_{15} is defined as the particle diameter below which 15% of the sand particles are smaller, $\tau_{RMS,c}$ is the standard deviation of the instantaneous critical wall shear stress.

In this study, the condition for the onset of motion is defined as $\tau_0 = \tau_{c,k}$ thus the critical characteristic wall shear stress can also be given by

$$\tau_{c,k} = 2(\text{Re}_c)^{-1}\rho U_{p,c}^2 \quad \text{with} \quad \text{Re}_c = \frac{U_{p,c}R_c}{\nu}$$

For nearly uniform sand, i.e., for $1/3 < d_{50}/d_{15} < 2$, the variation ratio $c_{v,d}$ varies from $1/4$ to $1/2$. For fines, Grass (1970) found $0.25 < c_{v,d} < 0.34$. If $c_{v,d} \rightarrow 0$ or $d_{15} \approx d_{50}$ then the sediment is uniform distributed or all particles are identical and if $c_{v,d}$ lies in the range of $1/2$ to 1 then the sediment is graded (or very graded).

If two materials, which have similar d_{50} , are considered, the fines, in the more graded material may be eroded first. This erosion process can easily be verified by using the Grass shear stress approach which is based on probability distributions. When the wall shear stress in laminar flow (spike function) is greater than the minimum critical wall shear stress (Gaussian function) the incipient motion starts, Figure 3 and when the wall shear stress is greater than the maximum critical wall shear stress general transport or the initiation of ripples occur.

Hence, the critical wall shear stress depends on both d_{15} and d_{50} . Based on more than 100 piping tests, Schmertmann (2000) found a strong correlation between the critical hydraulic dike gradient and d_{60}/d_{10} . Theoretically, a maximum critical wall shear stress and a minimum critical wall shear stress determine the transport of particles, so the erosion resistance is influenced not only by d_{60}/d_{10} , but also by d_{50} . Therefore, there is a limit to the range of soils to which the Schmertmann's relation applies.

In 2011, sand boils downstream of the dike near Vuren, a village along the Dutch river Waal, were observed and monitored. Soil samples showed that the sand close to the craters ($d_{50} = 0.09$ mm; $d_{70}/d_{15} \approx 2$) consisted of finer particles than the sand below the impermeable dike ($d_{50} = 0.26$ mm; $d_{70}/d_{15} \approx 3$, Van Beek et al. 2013). Hence, if sand is nearly uniform distributed then fines are transported earlier from the pipes to the sand boils.

However, the proposed equation for $\tau_{c,k}$ is not always valid, i.e. if the ratio between d_{90} and d_{10} is greater than 4 to 5 (e.g. Van Rijn 2014). For very graded sands, the finer particles are not representative for describing the initiation of motion as they could be locked between the coarser ones. In such cases, d_{50} or an upper limit, for example, d_{70} as proposed by Sellmeijer (1988) is recommended.

CRITICAL PIPE PARAMETERS

When particles upstream of the pipes fluidize, that is, if the mean hydraulic gradient upstream of the pipes exceeds the critical stage of heave then both pipe erosion and piping occur. However, these processes are also observed separately. Therefore, pipe erosion partly influences the piping

failure mechanism since transport of sand particles can occur in the unstable equilibrium phase. In that case, the pipe velocity, the pipe discharge and the hydraulic pipe gradient are larger than their critical values. For laminar flow conditions ($Re_* < 5$) the critical mean pipe velocity ($U_{p,c}$) reads

$$U_{p,c} = \sqrt{\frac{1}{2} Re_c \Psi_{\ell am,c} \left(\frac{\rho_s}{\rho} - 1 \right) g d_{15}}$$

Hence, $U_{p,c}$ depends on the critical Reynolds pipe number (Re_c), the critical wall shear velocity (through the critical Shields parameter, the relative density, the acceleration of gravity and the particle diameter) and the variation coefficient representing the influence of the non-uniformity.

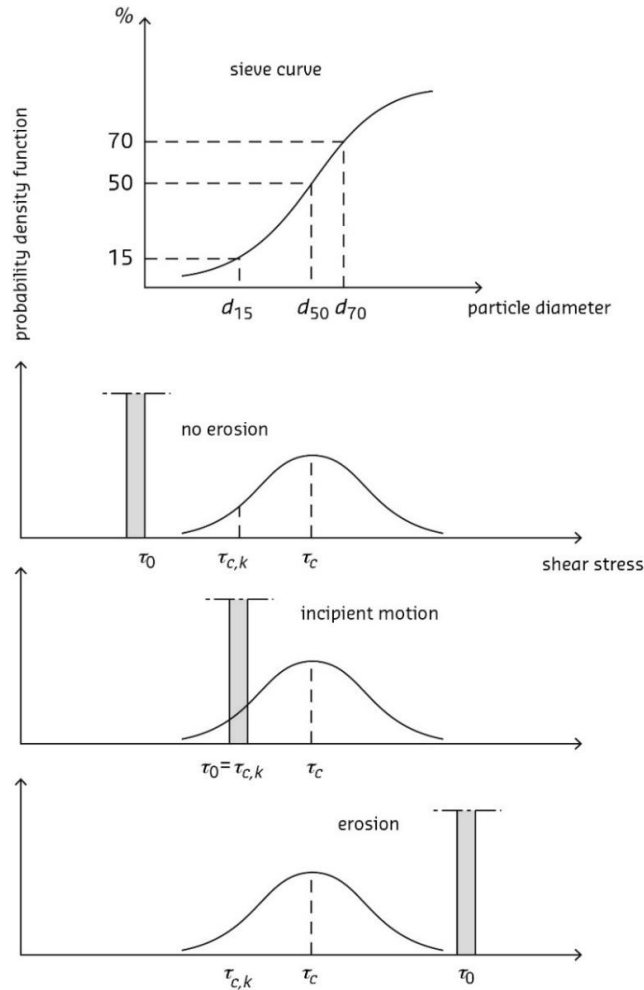


Figure 3. Shear-stress concept for laminar flow (analogous to Grass 1970)

Because the critical wall shear stress is constant the critical mean pipe velocities on the landside ($U_{p,m,c}$) is (subscripts m denotes on the landside)

$$U_{p,m,c} = \sqrt{\frac{1}{2} Re_{m,c} \Psi_{\ell am,c} \left(\frac{\rho_s}{\rho} - 1 \right) g d_{15}} \quad \text{with} \quad Re_{m,c} = \frac{U_{p,m,c} R_{m,c}}{\nu}$$

Based on the equation of continuity, the critical pipe discharge ($Q_{p,c}$) halfway along the pipes is

$$Q_{p,c} = A_{p,c} U_{p,c}$$

or with the definition of the Reynolds number

$$Q_{p,c} = \frac{A_{p,c} \text{Re}_c \nu}{R_c}$$

or with the definition of the hydraulic radius

$$Q_{p,c} = 2B_{p,c} \text{Re}_c \nu$$

Hence, the critical pipe discharge on the landside is

$$Q_{p,m,c} = 2B_{p,m,c} \text{Re}_{m,c} \nu$$

or per unit width

$$q_{p,m,c} = 2 \frac{B_{p,m,c}}{B} \text{Re}_{m,c} \nu = 2 \text{Re}_{m,c} \nu$$

The critical hydraulic pipe gradient can be presented by (halfway along the pipes for laminar flow conditions and if $d_{50}/d_{15} < 3$)

$$S_{pipe,c} = \frac{\Psi_{\ell am,c} \left(\frac{\rho_s}{\rho} - 1 \right) d_{15}}{R_c} = \frac{\Psi_{\ell am,c} \left(\frac{\rho_s}{\rho} - 1 \right) d_{15} U_{p,c}}{\nu \text{Re}_c} = \frac{\sqrt{g} \left(\Psi_{\ell am,c} \left(\frac{\rho_s}{\rho} - 1 \right) d_{15} \right)^{\frac{3}{2}}}{\nu \sqrt{2 \text{Re}_c}}$$

whence follows that $S_{pipe,c}$ depends on the pipe characteristics d_{15} , d_{50} (through $\Psi_{\ell am,c}$), Re_c , ρ_s , ρ and the temperature (through ν). The Reynolds number is important in analysing any type of flow when there is substantial velocity gradient (i.e. shear.). Usually the critical shear Reynolds number is written as

$$\text{Re}_{*,c} = \frac{d_{50} u_{*,c}}{\nu}$$

or with the definition of the critical bed shear velocity $u_{*,c} = (\tau_c/\rho)^{1/2}$

$$\text{Re}_{*,c} = D_*^{\frac{3}{2}} \sqrt{\Psi_{\ell am,c}}$$

If d_{50} varies from 0.1 mm ($\Psi_{\ell am,c} \approx 0.15$) to 0.5 mm ($\Psi_{\ell am,c} \approx 0.10$) with $\nu = 1.33 \cdot 10^{-6} \text{ m}^2/\text{s}$ it follows that $\text{Re}_{*,c} < 5$, yielding laminar flow conditions. However, for coarse sand (say 0.5 mm $< d_{50} < 5.0$ mm) the flow near the wall can be either laminar and / or turbulent as $5 < \text{Re}_{*,c} < 70$ and for gravel (say $d_{50} > 5.0$ mm) even turbulent.

APPLICATION OF THEORY

Laboratory experiments show that pipes below clayey dikes have wide rectangular or squeezed elliptic forms, in which the width-depth ratio ranges from 30 to 50. Van Beek (2015) found for Baskarp sand ($d_{50} = 0.13$ mm) that the critical pipe height ($\ell_{p,c}$) lies in the range of $2.5d_{50}$ to $7.5d_{50}$ (or $0.3 \text{ mm} < \ell_{p,c} < 1.0 \text{ mm}$). For Enschede sand ($d_{50} = 0.38$ mm) the measurements

showed that $1.5d_{50} < \ell_{p,c} < 3.0d_{50}$ (or $0.6 \text{ mm} < \ell_{p,c} < 1.2 \text{ mm}$) with a local maximum of $6d_{50}$ (or $\ell_{p,c} = 2.4 \text{ mm}$). Below some piping parameters are discussed for both fines and coarse sand.

According to Van Rijn (2014) the maximum pipe height that can be generated in a sand layer ($0.1 \text{ mm} < d_{50} < 0.5 \text{ mm}$) by erosion and transport processes is of the order of 2 mm. Larger pipe heights can hardly be developed as the applied wall shear stress is not large enough to generate sufficient particle movement. In other words, if the pipe height is higher than 2 mm then the vertical hydraulic gradient in the sand layer is insufficient large to discharge the required groundwater flow from the deep underlayers to the pipes. Moreover, the needed pipe length will not be achieved.

Considering fines ($d_{15} = 0.10 \text{ mm}$ and $d_{50} = 0.15 \text{ mm}$) with $\ell_{p,c} = 0.75 \text{ mm}$ (thus $\ell_{p,c}/d_{50} = 5$), $\Psi_{\ell_{am,c}} = 0.137$ and a wide rectangular pipe (thus $R_c = \frac{1}{2}\ell_{p,c}$) the following values of the piping parameters are obtained. The critical pipe velocity is 3.3 cm/s and thus the critical Reynolds number is about 10. The critical pipe discharge per unit width is 0.026 ℓ/s per m and the critical hydraulic pipe gradient is 0.056.

For coarse sand ($d_{15} = 0.30 \text{ mm}$ and $d_{50} = 0.50 \text{ mm}$) with $\ell_{p,c} = 1.0 \text{ mm}$ (thus $\ell_{p,c}/d_{50} = 2$), and $\Psi_{\ell_{am,c}} = 0.091$ it follows that the critical pipe velocity is 8.3 cm/s and thus the critical Reynolds number is 31. The critical pipe discharge per unit width is 0.083 ℓ/s per m and the critical hydraulic pipe gradient is 0.091.

For prototype conditions the critical dike gradient obtained from the Shields-Darcy model or the allowable hydraulic gradient equals about the critical hydraulic pipe gradient (this paper, see also Hoffmans and Van Rijn 2018 and Hoffmans 2020). Following Bligh (1910) the Creep factor equals for fines ($0.10 \text{ mm} < d < 0.15 \text{ mm}$) $1/0.056 = 18$ whence follows that the results of Shields-Darcy and Bligh are comparable. For coarse sand ($0.3 \text{ mm} < d < 2.0 \text{ mm}$) the Creep factor is $1/0.091 = 11$ which result is also comparable with the SD-model. Note that the aforementioned calculations concern best guess predictions, i.e. no safety factor has been included.

CONCLUSIONS

In this study the groundwater flow and the pipe flow are both laminar. Model relations are presented for the critical pipe velocity, critical pipe discharge and the critical hydraulic pipe gradient. They are all based on the approaches of Shields (1936) and Grass (1970) which describe the incipient motion of particles. If the sand is nearly uniform these relations can be used for predicting pipe erosion.

This study demonstrates that for prototype conditions the allowable hydraulic gradient as proposed by Bligh (1910) equals about the critical hydraulic pipe gradient obtained from the Shields-Darcy model for both fines and coarse sand ($0.1 \text{ mm} < d_{50} < 0.5 \text{ mm}$).

REFERENCES

- Bligh, W.G., 1910. Dams Barrages and weirs on porous foundations, Engineering News.
- Grass, A.J., 1970. Initial instability of fine bed sand, Hydraulic Division, Proc. of ASCE, Vol. 96, HY3, pp. 619-632.
- Hoffmans, G.J.C.M., 2012. The Influence of Turbulence on Soil erosion, Eburon, Delft.
- Hoffmans, G.J.C.M., Van Rijn, L.C., 2018. Hydraulic approach for predicting piping in dikes, Journal of Hydraulic Research, Vol. 56 (2).
- Hoffmans, G.J.C.M., 2020. Influence of erosion on piping in terms of field conditions, Journal of Hydraulic Research (to be published in July)
- Mantz, P. A., 1977. Incipient transport of fine grains and flakes by fluids — extended Shields diagram. Journal of Hydraulic Division, ASCE 103(HY6), 601-615.
- Schmertmann, F., 2000. The no-filter factor of safety against piping through sands, ASCE Geotechnical Special Publication No. 111. Judgement and innovation. Edited by F. Silva and E. Kavazanjian.
- Sellmeijer, J.B., 1988. On the mechanism of piping under impervious structures, Doctoral Thesis, Delft University of Technology (see also Deltares Publication No. 98, Delft).
- Shields, A., 1936. Anwendung der Aehnlichkeitsmechanik und der Turbulenzforschung auf die Geschiebebewegung, Mitteilungen der Preussischen Versuchsanstalt für Wasserbau und Schiffbau, Heft 26, Berlin NW 87.
- Van Beek, V. M., Yao, Q.L., Van, M.A., 2013. Backward Erosion piping model verification using cases in China and the Netherlands, Paper No. 3.29a, 7th Int. Conf. on Case Histories in Geotechnical Engineering and Symposium in Honor of Clyde Baker.
- Van Beek, V.M., 2015. Backward erosion piping: Initiation and progression, Doctoral Thesis, Technical University of Technology, Delft, The Netherlands.
- Van Rijn, L.C., 2014. Review of Piping Processes and Models, Report prepared for Deltares. www.leovanrijn-sediment.com.